Range-Doppler Radar Sensor Fusion for Fall Detection

Baris Erol[†], Moeness G. Amin[†] and Boualem Boashash[‡]
[†]Center for Advanced Communications
Villanova University, Villanova, PA, 19085, USA
[‡]Department of Electrical Engineering
College of Engineering, Qatar University, Doha, Qatar

***Abstract*—Falls are the major cause of accidents in the elderly population. Propelled by their non-intrusive sensing capabilities and robustness to heat and lighting conditions, radar-based automated fall detection systems have emerged as a candidate technology for reliable fall detection in assisted living. The use of a multiple radar system, in lieu of a single radar unit, for indoor monitoring combats occlusion and supported by the fact that motion articulations in the directions away from the line of sight generate weak Doppler signatures that are difficult to detect and classify. Fusion of the data from two radars is deemed to improve performance and reduce false alarms. Utilizing two 24 GHz ultra-wide band (UWB) radar sensing systems, we present different fusion architectures and sensor selection methods, demonstrating the merits of two-sensor platform for indoor motion monitoring and elderly care applications.**

I. Introduction

Recent studies have shown that people aged 65 and over represented 14.5% of the total population in 2014 and it is expected to grow to 21.7% by 2040 [1]. A considerable number of the elderly choose to exercise self-care within their homes, most of the time. One out of three elderly over the age 65 will fall every year which can result in injuries, reduced quality of life, and sometimes even death. Therefore, prompt assistance is crucial to reduce complications associated with a fall. Fall detection systems have been identified as a major innovation opportunity to improve the quality of elderly life. The main objective of a fall detection device is, upon fall, to alert and mobilize the first responders for an immediate and proper care and preventing long lying periods on the floor which can lead to hypothermia, dehydration, bronchopneumonia and pressure sores [2].

Recently, different types of fall detection systems have been proposed in the literature [3]–[5]. Most of the studies divide fall detectors into two main categories: wearable and non-wearable. The wearable devices are inexpensive but they have some major drawbacks, including the need to remember to wear them all times, and the push button devices require the elderly to be conscious after a fall. In this work, we focus on radar-based fall detection systems which are considered a sub-class of the non-wearable category. Various studies have shown that radar systems can be employed for reliable fall detection. Towards this goal, a plethora of fall motion features extracted from in single and joint-variable signal representations have been proposed [6]–[10].

The main challenge to radar fall detection is achieving low false alarms. One source of false alarms is the possible confusion of a fall with sitting and other sudden non-rhythmic motion articulations. The micro-Doppler signatures of sitting and falling might be similar, and this similarity may vary on a case-by-case basis. In many cases, the difference between two signatures in the time-frequency (TF) domain can prove insignificant, depending on how slow or fast each activity is. Therefore, range information can be employed in order to avoid mixing the two resembling motions: falling and sitting. Unlike falls, sitting has limited range extent which is determined by the depth of the chair used. Falls, on the other hand, can extend over a downrange that is approximately equal to the subject's height. In order to effectively reduce the miss-classification and false alarm rates, time-integrated range-Doppler maps were employed in [11]. The range-Doppler representation of the received signal combines both effects of the target velocity and range. Range-Doppler processing delivers fairly high resolution in both Doppler and range capable of resolving closely spaced targets with similar velocities. Time-integrated range-Doppler map is constructed by agglomeration of the consecutive range-Doppler frames. These maps offer Doppler signature properties while preserving the range information which is considered key in fall detection.

Target Doppler signature is sensitive to the direction of motion defined by the aspect angle, which is the angle between target motion trajectory and the radial path between the radar and the target [12], [13]. When the aspect angle approaches 90°, radar signal becomes strongly attenuated. The aspect angle impacts the quality of the extracted features, and as such, can impede fall classification. In one specific example, it is reported that the fall detection performance can drop approximately to below 50% for target directions with angles close to 90° [14]. For smaller aspect angles, it has been shown that classification performance will also degrade slightly and different levels. Multi-sensor approach could potentially overcome the aspect angle problem by placing the radars so that there is no blind spot and the target remains visible by one or the two radars, irrespective of motion orientation. Moreover, multi-sensor approach helps to resolve multiple targets in range. In multi-sensor approach, each sensor compliments less sensitive directions of the other sensors. The work in [15] proposed a decision fusion methodology based on the

978-1-4673-8823-8/17/$31.00 ©2017 IEEE

Choquet integral to combine the partial decision information acquired from each sensor. The feature level fusion and sensor selection methods were considered to correctly determine the fall event in [16]. In this paper, we examine the multi-sensor fusion methods and focus on three different levels of architectures: data level, feature level and decision level. In data level fusion, time-integrated range-Doppler maps acquired from each sensor, are fused by using simple averaging and Discrete Wavelet Transform (DWT). In feature level fusion, features of multiple sensors are simply concatenated together into a single feature vector. Extracted features should, however, be detectable in both sensors. In decision level fusion, soft decision outputs acquired from the k-Nearest Neighbors (kNN) and Support Vector Machine (SVM) for each sensor are combined using Bayesian fusion. In sensor selection, one sensor is selected based on the entropy metric which measures the information content of the time-integrated range-Doppler map. Upon selection, features are extracted and fall is classified by utilizing SVM.

The reminder of this paper is organized as follows. In Section 2, the UWB radar system and data experimental setup are introduced. In section 3, the feature extraction algorithm is provided. Different levels of multi-sensor fusion algorithms are discussed in Section 4. In Section 5, entropy-based sensor selection method is presented. In Section 6, experimental results for data-level fusion methods are provided and a performance comparison between single and multi-sensor methods is also presented. Finally, conclusions are drawn in Section 7.

II. Data Experimental Setup

The multi-sensor UWB radar experiments were conducted in the Radar Imaging Lab. at the Center for Advanced Communications, Villanova University. The UWB system used in the experiments, named SDRKIT 2500B, is developed by Ancortek, Inc. Operating parameters of the radar system: transmitting frequency 24 GHz, pulse repetition frequency (PRF) 1000 Hz, bandwidth 2 GHz which provides 0.075 m range resolution.

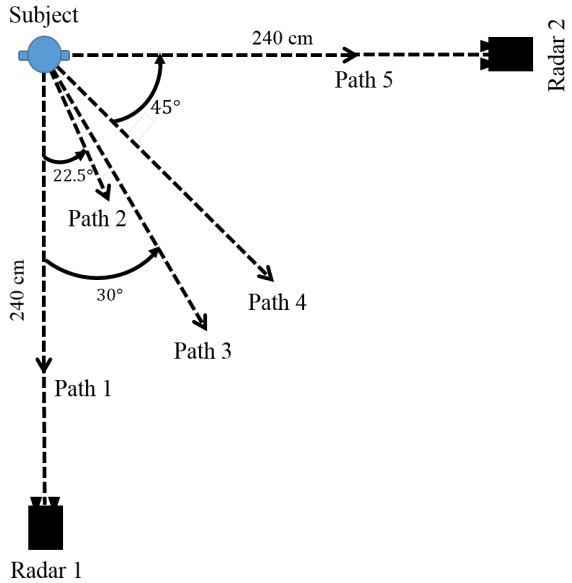

Fig. 1: Example configuration of the experimental setup

In this work, a radar network which consists of two UWB radars, placed on an L-shape geometry, is employed for the demonstration of the proposed multi-sensor fusion and selection algorithms. Null experiments were first conducted to investigate the impact of interference between sensors which helped in properly separating the two radars in the lab. Both radars are located 92 centimeters above the floor. The first radar was placed in the front side of the lab whereas the second radar was positioned at the right side of lab. An example configuration of the experimental setup is depicted in Fig. 1. Experiments were performed by 3 human subjects at a range of 240 centimeters away from both radars. The test subjects posed heights ranging from 1.75 to 1.76 m, weights ranging from 88 to 92 kg, and included 3 males. Four different motions are considered in the experiments: falling, sitting, bending, and walking. The micro-Doppler signatures, range vs slow time, and time-integrated range-Doppler maps are depicted in Fig. 2 for both falling and sitting motions where the aspect angle is 0 degrees. Motions were performed for 5 different directions as shown in the Fig. 1. This configuration allows to record simultaneous data with two angles, the sum of which is 90 degrees, for each motion direction. Each observation was recorded several times for a duration of 10 seconds, for 3 subjects, yielding a total of 320 data collections including all aspect angles from both sensors. Out of this number, 80 experiments corresponded to falling and the remaining experiments were related to other non-fall motions.

III. Feature Extraction

We defined our feature set as the area between the upper and lower envelope in the time-integrated range-Doppler map. Time-integrated range-Doppler map is constructed by agglomeration of the consecutive range-Doppler frames [11], [17]. Feature extraction approach is designed to take advantage of the target trajectory information in both range and Doppler. An energy-based thresholding algorithm is established to determine the outer envelopes (upper and lower) of the time-integrated range Doppler map from which the enclosed area feature can be extracted [18]. The feature extraction process is depicted in Fig. 3. First, the energy corresponding to the fast time index n is computed as

$$E(n) = \sum_{k=1}^{N} P(n,k), \quad n = 1, 2, ..., R \tag{1}$$

where $k = 1, 2, ..., N$ are the Doppler indices and $P(n,k)$ is the time-integrated range-Doppler map. For a selected fast time index n, the first frequency bin whose corresponding time-integrated range-Doppler value is greater than or equal to the product of a pre-determined threshold α and E is obtained. The pseudocode of the proposed envelope detection algorithm is provided below.

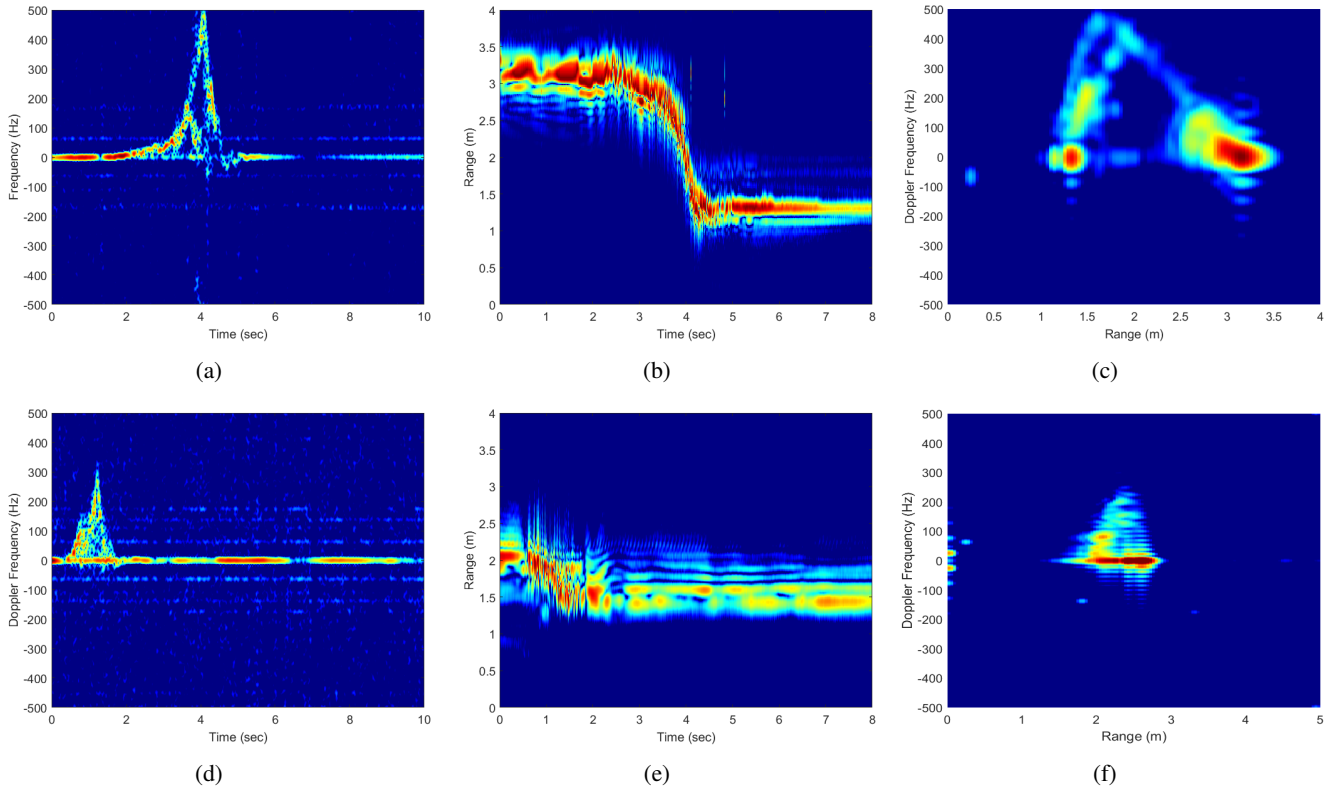

Fig. 2: Tri-domain representations of falling (a) Micro-Doppler signature (b) Range-slow time (c) Time-integrated range-Doppler map and tri-domain representations of sitting (d) Micro-Doppler signature (e) Range-slow time (f) Time-integrated range-Doppler map

The area captured in between the upper envelope f_U and the lower envelope f_L can be determined by implementing numerical integration methods, such as trapezoidal rule method [19]. This method approximates the integration over an interval by breaking it down into trapezoids with more easily computable areas. First, we determined the areas under the lower envelope A_L and upper envelope A_U separately:

$$A_L \approx \frac{R-1}{2R} \sum_{n=1}^{R} (f_L(n) + f_L(n+1)) \tag{2}$$

$$A_U \approx \frac{R-1}{2R} \sum_{n=1}^{R} (f_U(n) + f_U(n+1)) \tag{3}$$

Then, the area represented by the motion in this joint-variable domain can be found by subtracting A_U from A_L and taking the absolute value of the result.

IV. Multi Sensor Fusion

In recent years, multi-sensor fusion has received significant attention for radar-based automatic target recognition (ATR) systems. Fusion of data/information could be carried out on three different levels/architectures of abstraction closely interrelated with the flow of the classification process: data level, feature level, and decision level fusion [20].

The selection among these architectures is application specific and several considerations have to be made before implementing the fusion methods, such as characteristics of the sensors and availability of computational resources. In this paper, these architectures are discussed and applied to compare their respective fall detection performances.

A. Data Level Fusion

The first architecture, data level fusion, is a technique that mostly used in image processing applications. It combines

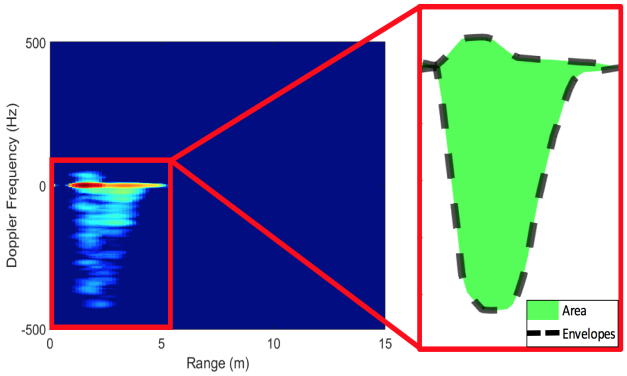

Fig. 3: Area feature extraction process

Algorithm 1 Envelope Detection

Input: $E(n)$, $P(n,k)$, α
Output: f_{env}, Outer Envelope Indices
Initialization
First LOOP Process
for $n = 1$ to R **do**
  $E_{th}(n) \leftarrow E(n) * \alpha$
  Second LOOP Process
  for $k = 1$ to N **do**
    $E_{temp} \leftarrow P(n,k)$
    if $\left(E_{temp} \geq E_{th}(n)\right)$ **then**
      $f_{env}(n) \leftarrow k$
      Return first loop
    end if
  end for
end for
return f_{env}

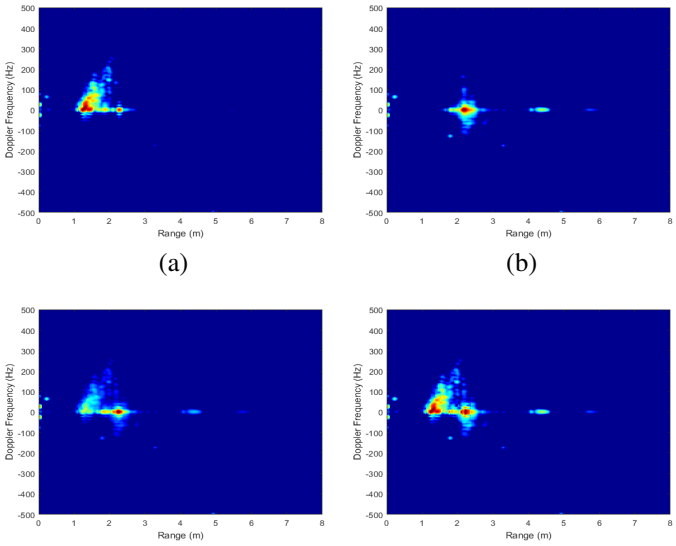

Fig. 4: Multi-sensor fall data for path 1 (a) Sensor 1 aspect angle: 0 degrees (b) Sensor 2 aspect angle: 90 degrees and data fusion results of (c) Simple average (d) DWT fusion

the registered images to increase the spatial resolution of low detail multi-sensor images while preserving their spectral information. In our case, data level fusion is utilized to regain the information that has been lost due to several reasons, such as aspect angle, target distance, and other types of environmental conditions. We consider two different data level fusion algorithms: simple averaging and DWT [21].

1) Simple Averaging Fusion: The simplest data level fusion method is to take an average of the gray level registered images, pixel by pixel. Averaging is a basic and straightforward process, and proceeds by simple averaging of the corresponding pixels in the two sensor images. However, this average fusion method may produce several undesired effects and reduce feature contrast which can lead to a degraded performance at the classification end of the system. The images acquired from sensor 1 and sensor 2 for path 1 can be seen in Fig 4-(a) and (b). The fused image of the time integrated range-Doppler maps is shown in Fig. 4-(c).

2) DWT Fusion: Wavelet theory has been extensively used in image processing to provide a multi-resolution decomposition of an image in a biorthogonal basis which results in a non-redundant image representation [21]. The basis functions are referred as wavelets and generated by the translation and dilation of mother wavelets. In wavelet analysis, the image or the signal is decomposed into scaled and shifted versions of the chosen mother wavelet functions. We employed the mother wavelet function as "Haar".

DWT separately filters and down samples the image in the vertical and horizontal directions. DWT provides low-high, high-low, high-high and low-low bands. The low-low band contains the average image information and can be seen as a smoothed and sub-sampled version of the registered image. Low-high, high-low and high-high bands are detailed sub images and they contain horizontal, vertical and diagonal information of the registered image, respectively. More formally, DWT decomposes an image recursively, depending on the decomposition level, into several frequency levels and each level contains transform values. After the nth level decomposition of the registered image, the output can be shown as

$$I_{n-1} = I_{LL_n} + I_{LH_n} + I_{HL_n} + I_{HH_n} \tag{4}$$

where I_{LL_n}, I_{LH_n}, I_{HL_n}, I_{HH_n} are the average image, vertical, horizontal and diagonal details of the decomposition, respectively. The nth level decomposition consists of $3n+1$ sub-image sequences. In DWT-based fusion scheme, the registered images (time-integrated range-Doppler maps) acquired from different sensors are decomposed separately. Then, the transformation coefficients of the sensor images are combined using a fusion rule, γ. The employed fusion rule takes average of the approximation coefficients and selects the detailed coefficients in each sub-band with the largest magnitude. The final fused image is generated by taking the inverse Discrete Wavelet transform (IDWT), and can be seen in Fig. 4-(d). It manifests good quality of the relevant information from the two different sensors.

B. Feature Level Fusion

The second architecture for multi-sensor fusion is called feature level fusion. In this case, each sensor provides the observational data, time-integrated range-Doppler maps, from which a feature vector is extracted. We define our feature set as the range-Doppler area. These feature sets are concatenated together into a single feature vector which represents an input to the SVM. The output of the classifier becomes a joint or fused declaration of motion identity based on the combined feature vector from the two sensors. Prior to integrating the feature vectors from individual sensors into a single larger

TABLE I: Performance evaluation metrics to compare the data-level fusion algorithms

	Fusion Mutual Information (MI)	Spatial Frequency (S_F)
Simple Average Fusion	0.2247	0.0109
DWT Fusion	0.2845	0.0279

TABLE II: Scores (%) for each method by 4 different metric

	Accuracy	Fall Detection Rate	False Alarm Rate	Missed Rate
Single sensor	66.84	40.21	6.52	59.79
Multi-Sensor data level fusion	91.63	87.81	4.54	12.19
Multi-Sensor feature level fusion	95.95	94.96	3.05	5.04
Multi-Sensor decision level fusion	79.63	65.79	6.52	34.21
Sensor Selection	86.99	79.84	5.84	20.16

feature vector, data alignment and association functions are applied to perform the multi-sensor task. Training scheme of the feature level fusion requires observations from both sensor.

C. Decision Level Fusion

The third and final architecture is called decision or classification level fusion. More generally, each sensor converts the range-Doppler information into a preliminary classification output. Decision level fusion can be divided into two general groups. The first group mostly focuses on the classifiers and puts emphasis on the development process of the classifier structure. On the other hand, the second group operates mainly on the decisions which are determined by separate classifiers. The decision level fusion methods (Bayesian fusion, fuzzy integrals, Dempster-Shaffer combination and etc.) attempt to reduce the level of uncertainty by optimizing the relation between the measures of evidence. For fall detection, the second group of decision level fusion methods have been considered in [15], with the application of Choquet integrals to improve the classification accuracy.

In this work, we focus on the fusion of soft outputs produced by classifiers. Decision fusion methodology involves two UWB radar sensors and two classifiers (kNN, and SVM). Simple Bayes average fusion was employed in order to improve fall detection rate where the target signatures were severely attenuated by the aspect angle. However, Bayesian methods can only applied to the soft outputs expressed in posterior probabilities. Standard SVMs do not provide the calibrated posterior probabilities to enable decision fusion. Therefore, when the classes are not perfectly separable, an additional sigmoid function can be employed to map the SVM classification outputs into probabilities [9]. kNN provides the classification results in posterior probabilities so it does not need any extra function. The example diagram of the decision-level fusion based fall detection system is depicted in Fig. 5.

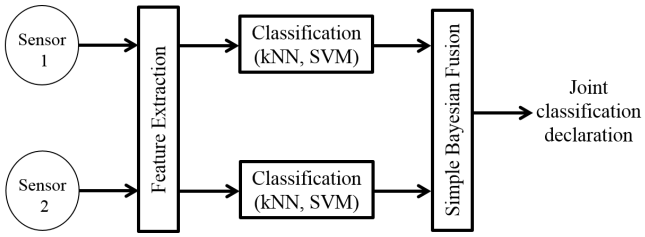

Fig. 5: The diagram of decision level fusion

V. Sensor Selection

The main difference between single sensor and multi-sensor systems manifests itself in the dependency on the aspect angle. Thus, one of the main tasks of a multi-sensor system is to determine the sensor that provides sufficient information for classification decisions. Sensor selection could be carried out in several ways. For fall detection, the power spectral density (PSD) of a specific Doppler bandwidth, which categorizes the motion, has been used in [16].

In this work, an entropy-based selection method is utilized to measure the quality of the time-integrated range-Doppler maps obtained from each sensor. Generally, entropy metrics are used to measure the information content of an image. Therefore, range-Doppler map with high information content will proportionally have high entropy. We implemented the Rényi entropy which quantifies the uncertainty of underlying distribution and it can be easily adopted for quantifying the complexity or randomness of time-integrated range-Doppler maps [22]. Rényi entropy is defined as

$$H_\alpha = \frac{1}{1-\alpha}\log_2 \sum_n \sum_k \left(\frac{P(n,k)}{\sum_n \sum_k P(n,k)} \right)^\alpha \qquad (5)$$

where α is the order of the entropy and it takes values between 0 and 1. $P(n,k)$ is the time-integrated range-Doppler map. It is noted that large values of α enhance the peaks in the entropy profile of the image while smoothing out some of the local details, whereas lower α values are not as discriminative [23]. The most important drawback of the Réyni entropy is sensitivity to noise and other types of unwanted rapid fluctuations.

The Rényi entropy offers a metric of the contribution of a given sensor to the classification problem. Thus, the sensor with the highest Rényi entropy is selected for the feature extraction and classification process.

VI. Experimental Results

In this section, single sensor, four aforementioned fusion and sensor selection methods were compared. SVM classifier

with a radial basis kernel function was utilized. 60% of the recorded signals were used for training the classifier, whereas the remaining 40% were used as testing. Data for training and test samples were selected in a random fashion, and 1000 Monte Carlo trials were conducted.

The performance comparison between data-level fusion methods (simple average and DWT) is obtained by computing the quality assessment metrics: fusion mutual information and spatial frequency, as tabulated in Table 1. The spatial frequency measures the overall activity level of the fused image [24]. High value of spatial frequency indicates that the fused image contains important information from both images. The degree of dependency between input and fused image is computed by fusion mutual information [25]. Larger value of this metric indicates a better quality. From these metrics, a number of important observations can be made. It is observed that simple averaging method exhibits a degraded fusion performance in every metric. This can be explained by the artifacts and noise effects that are formed after the addition of the two registered images. On the other hand, DWT-based fusion provides the better performance which is anticipated due to higher level of decomposition and noise filtering properties of the DWT. Therefore, we only used DWT fused images for feature extraction and classification.

In Table 2, accuracy, fall detection rate, false alarm rate and missed rate are provided for single-sensor, multi-sensor fusion methods (data, feature and fusion level) and sensor selection. The single sensor fails to provide desirable detection performance because of the angle dependency as expected. On the other hand, the data-level fusion method provides an acceptable level of classification accuracy at 91.63%. Decision-level fusion yields 79.63% accuracy which can be explained by the simplicity of the fusion method. Sensor selection also provides an acceptable level of accuracy at 86.99%. Finally, the feature level fusion method provides the highest accuracy, fall detection rate and the lowest false alarm and missed rate.

VII. Conclusion

With the shortcomings of a single radar unit fall classifier, this paper puts forward a multi-sensor based fall detection system with different levels of data fusion and sensor selection. Two UWB radar sensors were used for the generation of time-integrated range-Doppler maps. Multi-sensor fusion architectures and sensor selection methods were discussed. It was shown that the DWT fusion method outperforms the simple averaging fusion. Finally, classification performance comparison was presented between single-sensor, multi-sensor fusion methods and sensor selection. It was demonstrated that feature level fusion provides the best performance.

ACKNOWLEDGEMENT

This paper is made possible by NPRP Grant # NPRP 6-680-2-282 from the Qatar National Research Fund (a member of Qatar Foundation). The statements made herein are solely the responsibility of the authors.

References

[1] J. A. Stevens, "Fatalities and injuries from falls among older adults - united states, 1993-2003 and 2011-2005," *MMWR*, vol. 55(45), 2006.

[2] M. E. Tinetti, W. L. Liu, and E. B. Claus, "Predictors and prognosis of inability to get up after falls among elderly persons," *JAMA*, vol. 269, no. 1, pp. 65–70, 1993.

[3] R. Igual, C. Medrano, and I. Plaza, "Challenges, issues and trends in fall detection systems," *Biomed Eng Online*, vol. 12, no. 66, pp. 66, 2013.

[4] M. G. Amin, *Radar for indoor monitoring*, CRC Press, 2017.

[5] F. Ahmad, A. Cetin, K. Ho, and J. E. Nelson, "Special section on signal processing for assisted living," *IEEE Signal Processing Magazine*, vol. 33, no. 2, pp. 71–80, 2016.

[6] M. G. Amin, Y. D. Zhang, F. Ahmad, and K. C. Ho, "Radar signal processing for elderly fall detection: The future for in-home monitoring," *IEEE Signal Processing Magazine*, vol. 33, no. 2, pp. 71–80, 2016.

[7] Q. Wu, Y. D. Zhang, W. Tao, and M. G. Amin, "Radar-based fall detection based on doppler time-frequency signatures for assisted living," *Sonar Navigation IET Radar*, vol. 9, no. 2, pp. 164–172, 2015.

[8] B. Y. Su, K. C. Ho, M. J. Rantz, and M. Skubic, "Doppler radar fall activity detection using the wavelet transform," *IEEE Transactions on Biomedical Engineering*, vol. 62, no. 3, pp. 865–875, 2015.

[9] B. Erol, M. G. Amin, Z. Zhou, and J. Zhang, "Range information for reducing fall false alarms in assisted living," in *2016 IEEE Radar Conference (RadarConf)*, Philadelphia, PA, 2016, IEEE, pp. 1–6.

[10] B. Jokanovic, M. G. Amin, and F. Ahmad, "Radar fall motion detection using deep learning," in *2016 IEEE Radar Conference (RadarConf)*, Philadelphia, PA, 2016, pp. 1–6.

[11] B. Erol and M. G. Amin, "Fall motion detection using combined range and doppler features," in *2016 24th European Signal Processing Conference (EUSIPCO)*, Budapest, 2016, pp. 2075–2080.

[12] F. Fioranelli, M. Ritchie, and H. Griffiths, "Aspect angle dependence and multistatic data fusion for micro-doppler classification of armed/unarmed personnel," *Sonar Navigation IET Radar*, vol. 9, no. 9, pp. 1231–1239, 2015.

[13] M. Vespe, C. J. Baker, and H. Griffiths, "Radar target classification using multiple perspectives," *Sonar Navigation IET Radar*, vol. 1, no. 4, pp. 300–307, 2007.

[14] B. Erol and M. G. Amin, "Effects of range spread and aspect angle on radar fall detection," in *2016 IEEE Sensor Array and Multichannel Signal Processing Workshop (SAM)*, Rio de Janerio, 2016, pp. 1–5.

[15] L. Liu, M. Popescu, M. Rantz, and M. Skubic, "Fall detection using doppler radar and classifier fusion," in *Proceedings of 2012 IEEE-EMBS International Conference on Biomedical and Health Informatics*, Hong Kong, 2012, pp. 180–183.

[16] S. Tomii and T. Ohtsuki, "Learning based falling detection using multiple doppler sensors," *Advances in Internet of Things*, vol. 3, pp. 33–43, 2013.

[17] D. Tahmoush and J. Silvious, "Time-integrated range-doppler maps for visualizing and classifying radar data," in *2011 IEEE RadarCon (RADAR)*, Kansas City, MO, 2011, pp. 372–374.

[18] B. Erol, M. G. Amin, F. Ahmad, and B. Boashash, "Radar fall detectors: a comparison," in *Proc. SPIE 9829, Radar Sensor Technology XX*, Baltimore, MD, 2016.

[19] K. E. Atkinson, *An introduction to numerical analysis*, John Wiley and Sons, 1989.

[20] D. L. Hall and J. Llinas, "An introduction to multisensor data fusion," *Proceedings of the IEEE*, vol. 85, no. 1, pp. 6–23, 1997.

[21] J. R. Raol, *Multi-Sensor data fusion with MATLAB*, CRC Press, 2010.

[22] S. Aviyente and W. J. Williams, "Minimum entropy time-frequency distributions," *IEEE Signal Processing Letters*, vol. 12, no. 1, pp. 37–40, 2005.

[23] S. Aviyente, F. Ahmad, and M. G. Amin, "Information theoretic measures for change detection in urban sensing applications," in *2007 IEEE Workshop on Signal Processing Applications for Public Security and Forensics*, Washington, DC, USA, 2007, pp. 1–6.

[24] V. P. S. Naidu and J. R. Raol, "Pixel-level image fusion using wavelets and principal component analysis," *Defense Science Journal*, vol. 33, no. 2, pp. 71–80, 2016.

[25] P. Jagalingam and A. V. Hegde, "A review of quality metrics for fused image," *Aquatic Procedia*, vol. 4, pp. 133 – 142, 2015.